Evaluation of the capability of the RANS turbulence model to account for the effects of the variations of the nozzle condition for a round free jet flow

Gylles Ricardo Ströher, gylles@utfpr.edu.br
Universidade Tecnológica Federal do Paraná, End.: R. Marcílio Dias, 635, CEP 86812-460 – Apucarana – PR – Brasil

Rosiane Cristina Lima, rosiane@ita.br
Cláudia Regina de Andrade, claudia@ita.br
Edson Luiz Zaparoli, zaparoli@ita.br
Instituto Tecnológico de Aeronáutica, End.: Praça Marechal Eduardo Gomes, 50 - Vila das Acácias CEP 12228-900 – São José dos Campos – SP – Brasil

Abstract. *During the past years the development of more accurate, efficient and robust turbulence models have been significant. Different turbulence models in conjunction with Reynolds Averaged Navier Stokes (RANS) are available in Computational Fluid Dynamics (CFD) codes to predict complex flow features. The evaluation of turbulence models performance in simpler flows can provide important information for more complex problem. Free jet flow is a fundamental fluid mechanical benchmark problem to validate turbulence models predictions. In this work the turbulence model capability to predict the influence on the downstream flow caused by variations in the jet origin conditions is assessed. The incompressible axysimmetric turbulent free jet was solved numerically using three RANS based turbulence models: standard k-ε, realizable k-ε and v2-f. The numerical results have been compared with experimental data available in current literature for two jets issuing from a nozzle with fully-developed and "top-hat" velocity profile. Governing equations (mass conservation, momentum, energy and turbulence model) are discretized employing the finite volume method with a segregated solver and second order discretization approach. Results obtained using the two tested k-ε turbulence models presented good agreement with experimental ones with "top-hat" jet inlet (origin) boundary condition and* the Rans turbulence models tested can account for the effect of the source for the downstream flow, however the models are not able to predict the correctly quantitative levels.

Keywords*: Free Jet, RANS Turbulent Model, Computational Fluid Dynamic*

1. INTRODUCTION

The flow structure of an incompressible free jet is given in Fig. 1. In this case there are three distinct regions in the flow the potential core, the developed region and region in between, named transition region. In potential core region, the centerline axial mean velocity is constant. As the shear layers meet, the jet undergoes a transition into the fully developed regime. In the fully developed region, the jet is self-preservation. This means that profiles of a flow quantity, such as axial mean velocity, taken at different downstream distances, will all collapse when properly scaled (Pope 2000).

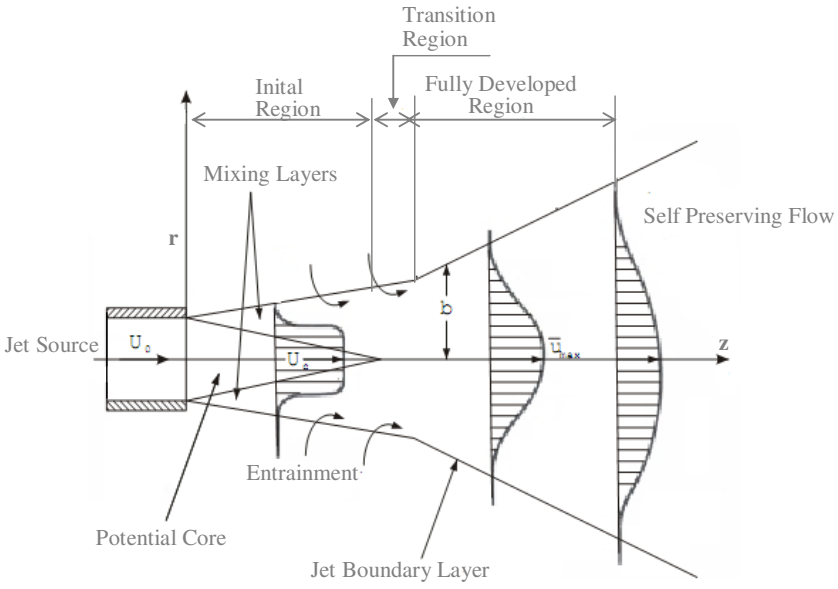

Figure 1. Schematic of an axisymmetric free jet. (White, 1991).

Self-preservation, also called self-similarity, is a very interesting feature of flows in which the flow properties depend on one variable only. The self similar regime is established a few nozzle diameters downstream the nozzle exit, regardless of its initial conditions; though they will influence the location at which the self similar region starts.

Because of the large number of old experimental studies in self-similarity region, the hypothesis was established in the past that a turbulence "forget its origins" in the case that the flow can be considered two-dimensional or axysimmetric.

However, the analytical results of George (1989), and subsequently George and Davidson (2004), dispelled this hypothesis by showing that the entire flow is influenced by the initial (or upstream) conditions, resulting in a variety of initial-condition-dependent self-similar states in the far field. George and Davidson (2004) discuss that the single point turbulence models (RANS) lack the necessary physics to be able to account for the asymptotic effect of the initial conditions.

Among the RANS models, the standard k-ε of Launder et al (1976) is one of the most widely utilized turbulence for various turbulence flows of engineering interest. This model presents the well-known round-jet anomaly (named based on the finding that the spreading rate in planar jets is predicted reasonably well, but prediction of the spreading rate for axisymmetric jets is unexpectedly poor), which is considered to be mainly due to the modeled dissipation equation.

Wilcox (1994) compared the spreading rate of plane jet and round free jet predicted by the standard k-ε turbulence model. Only for the plane jet the standard k-ε predicted spreading rate falls within the range of measured values. However, its predicted spreading rate is 25% to 40% higher than that measured for the round jet. In order to improve the ability of the standard k-ε to predict complex turbulent flows, Shih et al (1995) proposed a realizable k-ε that has a new formulation for both the model dissipation rate equation (ε) and the eddy viscosity that can significantly improve the performance of the standard k-ε model for round free jets.

An attractive alternative to the k-ε two-equation models is the *v2-f* turbulence model developed by Durbin (1995). According to Durbin (1995), this model has the advantage of having fewer equations than the Reynolds Stress model and yet it is numerically more robust. Another important feature is that the *v2-f* model considers the scale turbulence limited by Kolmogorov scale (υ/ε) and (k/ε) whilst the k-ε models consider only large scales (k/ε).

In this work, the capability of the three RANS turbulence models (standard k-ε, realizable k-ε and *v2-f)* to predict the influence on the downstream flow caused by variations to the nozzle source flow in turbulence levels is assessed. The numerical results are compared with experimental data available in current literature for two jets issuing from a long pipe (developed velocity profile) and one from a smooth contraction ('top hat' velocity profile).

2. MATHEMATICAL FORMULATION

The system in the present study is the air jet emerging into an initially stagnant air surrounding. The flow field is incompressible, stead steady, axisymmetric and turbulent. The governing Reynolds-averaged transport (RANS) equations can be given in the following form:

Continuity equation:

$$\nabla \cdot U = 0 \tag{1}$$

Momentum equation:

$$U \cdot \nabla U = -(1/\rho)\nabla P + \nabla \cdot \left[\left(\upsilon + \upsilon_t \right) \nabla U \right] \tag{2}$$

where ρ is the density, U is the Reynolds-averaged velocity vector, P is the Reynolds-averaged pressure, υ is the dynamic molecular viscosity, and υ_t is the turbulent viscosity.

In order that the mean flow equations can be closed, the turbulent viscosity υ_t was computed using the followings RANS turbulence models: two equations standard k - ε of Launder e Spalding (1972), realizable k - ε of Shih et al. (1995) and the four equations the *v2-f* model of Durbin (1995).

2.1 RANS Turbulence Models

In the k-ε standard model, the eddy viscosity is computed using the relation:

$$\upsilon_t = \frac{\mu_t}{\rho} = C_\mu \rho \frac{k}{\varepsilon} \tag{3}$$

Where: C_μ is a constant and the values of k and the dissipation, ε, come from the solution of the transport equations. The k-equation (Eq. 4) is derived by subtracting the instantaneous mechanical energy from its time averaged value, and the ε-equation (Eq. 5) is formed from physical reasoning.

$$\rho u_i \frac{\partial k}{\partial x_i} = \frac{\partial}{\partial x_i}\left(\mu + \frac{\mu_t}{\sigma_k}\right)\frac{\partial k}{\partial x_i} + P_k - \rho\varepsilon \tag{4}$$

$$\rho u_i \frac{\partial \varepsilon}{\partial x_i} = \frac{\partial}{\partial x_i}\left(\mu + \frac{\mu_t}{\sigma_k}\right)\frac{\partial \varepsilon}{\partial x_i} + P_k + \frac{\varepsilon}{k}\left(C_{\varepsilon 1} P_k - C_{\varepsilon 2}\rho\varepsilon\right) \tag{5}$$

The turbulence production term, P_k, is modeled using:

$$P_k = \mu_t \frac{\partial u_i}{\partial x_i}\left(\frac{\partial u_i}{\partial x_i} + \frac{\partial u_j}{\partial x_i}\right) \tag{6}$$

The values for the standard k-ε equation constants used in this work are $C_\mu = 0.09$, $C_{\varepsilon 1} = 1.45$, $C_{\varepsilon 2} = 1.9$, $\sigma_k = 1.0$, and $\sigma_\varepsilon = 1.3$.

In the realizable k-ε model, the eddy viscosity is computed like the standard k-ε model, but C_μ isn't constant. It is computed from:

$$C_\mu = \frac{1}{A_0 + A_S \dfrac{kU^\bullet}{\varepsilon}} \tag{7}$$

where

$$U^\bullet \equiv \sqrt{S_{ij}S_{ij} + \tilde{\Omega}_{ij}\tilde{\Omega}_{ij}}\ , \quad \tilde{\Omega}_{ij} = \Omega_{ij} - 2\varepsilon_{ijk}\omega_k\ , \qquad \Omega_{ij} = \overline{\Omega_{ij}} - \varepsilon_{ijk}\omega_k \tag{8}$$

where $\overline{\Omega_{ij}}$ is the mean rate-of-rotation tensor viewed in a rotating reference frame with the angular velocity ω_k. The model constants are $A_0 = 4.04$, $A_S = \sqrt{6}\cos\phi$, where:

$$\phi = \frac{1}{3}\cos^{-1}\left(\sqrt{6}W\right), \quad W = \frac{S_{ij}S_{ik}S_{ki}}{\tilde{S}}, \quad \tilde{S} = \sqrt{S_{ij}S_{ij}}\ , \quad S_{ij} = \frac{1}{2}\left(\frac{\partial u_j}{\partial x_i} + \frac{\partial u_i}{\partial x_j}\right) \tag{9}$$

The k-equation for this turbulence model is the same of standard model. However the ε-equation is different. Shih et al. (1995) proposed a new model dissipation rate equation (Eq. 11) that is based on the dynamic equation of the mean-square vorticity fluctuation at large turbulent Reynolds number.

$$\rho u_i \frac{\partial \varepsilon}{\partial x_i} = \frac{\partial}{\partial x_i}\left(\mu + \frac{\mu_t}{\sigma_k}\right)\frac{\partial \varepsilon}{\partial x_i} + \rho C_1 S_\varepsilon - \rho C_2 \frac{\varepsilon^2}{k + \sqrt{v\varepsilon}} S_\varepsilon \frac{\varepsilon}{k}\left(C_{\varepsilon 1} P_k - C_{\varepsilon 2}\rho\varepsilon\right) \tag{10}$$

The values for the realizable k–ε equation constants used in this work were $C_{1\varepsilon} = 1.44$, $C_{2\varepsilon} = 1.9$, $\sigma_k = 1.0$ and $\sigma_\varepsilon = 1.2$.

The *v2-f* turbulence model is based in another eddy viscosity equation

$$\mu_t = C_\mu \overline{v^2}\frac{k}{\varepsilon} \tag{11}$$

where C_μ is usually 0.2.

The *v2-f* uses v^2 as an additional velocity scale, elliptic relaxation, which accounts for non-viscous wall blockage effects, and a switch of the scales from energy-containing to Kolmogorov, to account for viscosity effects very close to

a wall. Therefore it solves two additional equations in comparison with the standard k– ε model, i.e. a transport equation for v^2 and an elliptic equation for the elliptic relaxation parameter f. The v^2 and f equations are the followings.

$$\rho\frac{\partial\overline{v^2}}{\partial x_i}=\frac{\partial}{\partial x_i}\left[\left(\mu+\frac{\mu_t}{\sigma_\varepsilon}\right)\frac{\partial\overline{v^2}}{\partial x_i}\mu\right]+kf\frac{\overline{v^2}}{k}\varepsilon \tag{12}$$

$$f=L^2\frac{\partial f}{\partial^2 x_i}+(C_1-1)\frac{(2/3-\overline{v^2}/k)}{\mathrm{T}}+C_2\frac{P_k}{k} \tag{13}$$

The values for the *v2-f* equation constants used in this work are $C_{1\varepsilon}=1.44$, $C_{2\varepsilon}=1.9$, $\sigma_k=1.0$ and $\sigma_\varepsilon=1.2$.

2.2. Computational Domain and Boundary Conditions

The geometry used to model the free jet problem is shown in Figure 2. Five boundary conditions need to be considered, including: unbounded air outlet (pressure outlet), symmetry axis, solid wall and inlet.

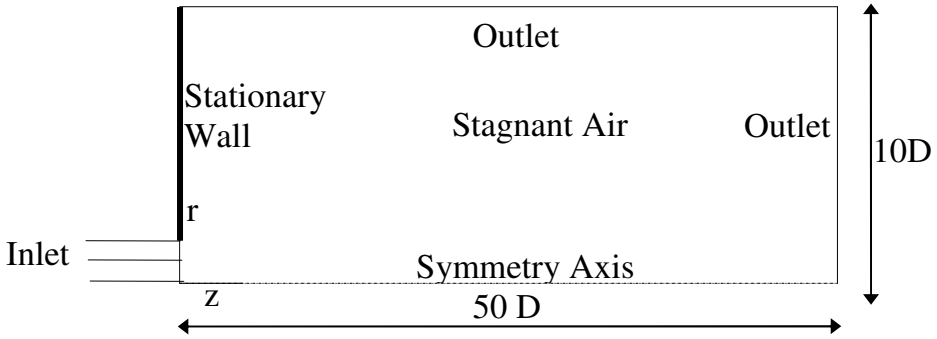

Figure 2. The solution domain and boundary conditions (drawing without scale).

Outlet Conditions

It is considered that the flow extends over a sufficiently long domain so that the pressure boundary is satisfied. Thus the pressure is the same as ambient.

Solid Wall

At a solid boundary the no-slip condition was applied so that both mean and fluctuating velocities are zero but the dissipation rate is infinite.

Symmetry Axis

At a symmetry axis the radial derivatives for all mean variables, except the radial velocity was steed to zero.

Inlet Conditions

Two inlet velocity conditions were specified: 'top-hat' and developed velocity profile. We used the experimental data from Frost and Jambunathan (1996) and Mi et al. (2001a). Table 1 summarizes the inlet conditions case name, author that provides experimental data, velocity profile and the Reynolds Number based on nozzle exit conditions.

Table 1. Simulated Cases

Case	Experimental Data	Velocity Profile	Re_0
I	Frost and Jambunathan (1996)	'top-hat'	22,500
II	Frost and Jambunathan (1996)	developed, n=6.5	22,500
III	Mi et al. (2001a)	developed, n =6.62	28,200

For Cases I and II, the velocity profiles may be approximated by the equation $U/U_{center} = (1\text{-}2r/D)^{1/n}$, where n is given in Table 1. The intensity turbulence for the three cases at the exit nozzle is given in Figure 3. The turbulence boundary conditions for k and ε were calculated using the values in Fig. 3 and the Eq. 14 (a) and (b).

$$k = \frac{3}{2}\left(U_{avg} I\right)^2 \text{ (a)} \quad \varepsilon = C_\mu^{3/4} \frac{k^{3/2}}{l} \text{ (b)} \quad l = 0.07 D_h \text{ (c)} \tag{14}$$

where length scale l represents the large scale turbulence, I is turbulence intensity, D_h is hydraulic diameter, and C_μ is an empirical constant (typically 0.09).

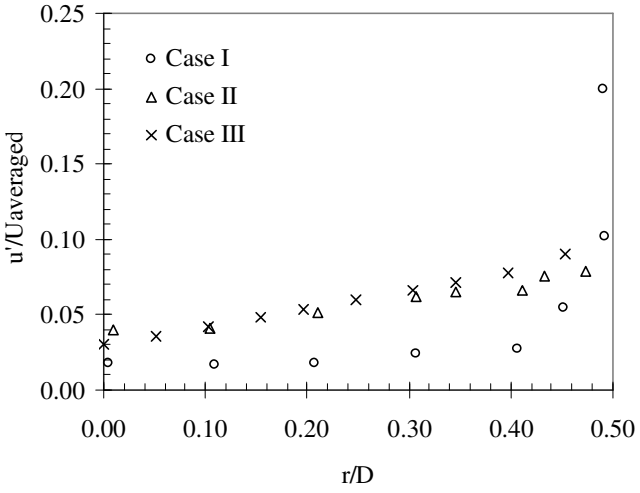

Figure 3. Turbulence characteristics of the fully developed and flat jet exit profiles.

Case I and Case II have the same Reynolds number (Re_0) based on jet initial conditions. Mi et al. (2001b) showed if $(Re_0)_{developed} = (Re_0)_{top\text{-}hat}$ and the same jet fluid is used, the jet initial moment $(J)_{developed}$ is only slightly greater (1.2-2.8%) than $(J)_{top\text{-}hat}$. In other words, the same Re_0 used for the two jets can lead to nearly identical momentum addition rates, for Case I and II: $(J)_{CaseI} = 2.4\%(J)_{CaseII}$.

3. SOLUTION STRATEGIES

The axisymmetric turbulent flow field was calculated by solving the Reynolds Averaged Navier-Stokes (RANS) and turbulence models equations available in a CFD package (FLUENT 6.3). The equations are discretized by finite volume method and solved using the "uncoupled" solver and convective terms discretized using the spatial second order scheme (Barth and Jespersen, 1989). The pressure-velocity coupling algorithm used was SIMPLEC (Vandoormaal and Raithby, 1984). Solutions were considered converged when the maximum residual of all the discretized equations was less than 1×10^{-5} and when the total momentum in z direction remained constant and independent of the distance z from the nozzle.

Structured and uniform grids were generated for the solution domain shown in Figure 2. Mesh independence tests were performed using three computational grids with the following cell numbers 30,000 (coarse), 60,000 (medium), and 100,000 (fine). The maximum differences in the centerline velocity (along the z axis) between the coarse and medium grids, and between the medium and the fine grids, were less than 0.5% and 0.05%, respectively (within typical experimental error range). Based on these results, the medium grid was selected for all computations in the present investigation.

4. RESULTS AND DISCUSSION

Numerical results were obtained from an air free discharge that had the same parameters as a jet that was experimentally tested by Frost and Jambunathan (1996), Case I. The centerline dimensionless axial velocity decay (V/V_0, V_0 = centerline velocity at nozzle exit) is shown starting from the nozzle exit (corresponding to inlet in Fig. 2). Figure 4 shows the centerline dimensionless velocity decay obtained from the standard and realizable k– ε models and the *v2-f* turbulence model.

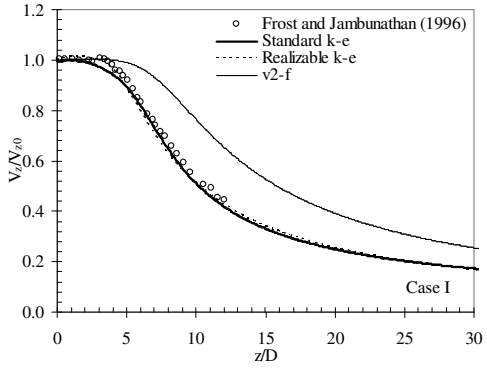

Figure 4. Case I - Normalized mean axial velocity on symmetry axis vs. normalized distance from nozzle exit, calculation results of three tested turbulence models.

Figure 4 shows that numerical solutions obtained with the *k–ε* models were similar and a good agreement can be seen between the profile measured by Frost and Jambunathan (1996) and the *k– ε* numerical results. However, the *v2-f* model does not satisfactorily predict the behavior of the jet velocity axial decay. The *v2-f* model evaluated an unreal long length for potential core region and high level of the velocity at the fully developed region. Thus, results indicate that the mixture rate predicted using *v2-f* was lower than the *k–ε* models; therefore, the jet momentum lost for the stagnant fluid was underestimated.

Since Frost and Jambunathan's (1996) work did not provide data for the radial velocity decay, the numerical results were compared with Schilichting's (1979) data in the development region where the self-preservation is established. This can be seen in Fig. 5 and further information about the self-preservation profile can be obtained from George (1989) and Pope (2005).

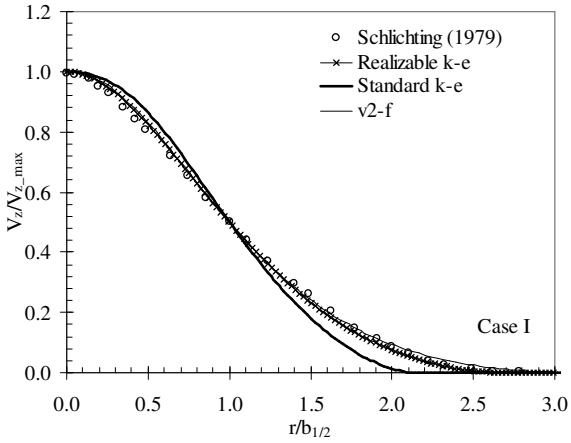

Figure 5. Case I - Normalized mean axial velocity against dimensionless radial distance.

Results of the *v2-f* and the realizable *k–ε* models agreed well with the self-preservation profile, whilst the standard *k–ε* provides good results only when $r/b_{1/2} < 1.2$. This behavior of the standard *k-ε* was expected due to its well known inability to predict the jet spreading rate as mentioned by Pope (1978).

Results shown in Figs. 4 and 5 indicated that to validate a turbulence model only by checking its solution against the self-preservation profile can lead to wrong conclusions about the performance of the studied model. In the present work, this is evidenced by the results obtained from the standard and the *v2-f* models. The first one presented good results for the axial velocity decay, and the second one provided good results when compared with the self-preservation profile.

Numerical results were also obtained from a free air jet with similar conditions experimentally tested by Frost and Jambunathan (1996) and Mi et al. (2001a), Case II and Case III, respectively. Figure 6 shows the centerline dimensionless axial velocity decay predicted by the standard and realizable k– ε models and the *v2-f* turbulence model.

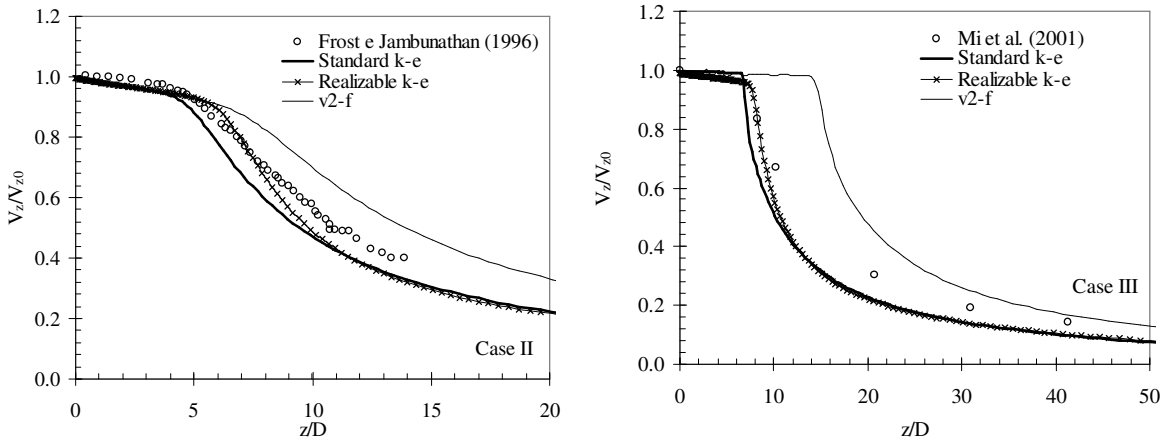

Figure 6. Case II and Case III - Normalized mean axial velocity on symmetry axis vs. normalized distance from nozzle exit results of the three tested turbulence models.

Note that experimental axial velocity profile decays immediately after the nozzle exit, so the potential core length is too small. With the exception of the *v2-f* model (which predicted a long unreal potential length), the *k-ε* turbulence models predicted higher decay velocity than the experimental data. The two *k-ε* turbulence models evaluated a more intense loss momentum than the experimental free jet behavior.

Additionally, results about the prediction of the turbulence model for turbulent kinetic energy (*k*) are given in Fig. 7. The intensity of turbulence immediately after the nozzle increases due to the shear layer of the neighboring fluid. This layer grows at the center line of the jet further increasing the intensity of turbulence. The three models predicted this behavior, but neither quantitatively agreed well with experimental data.

In the beginning, approximately when z / D = 4, the effect of the turbulent mixing layer is small and the three turbulence models have the same profile of turbulence intensity, though lower than the experimental data. After z / D = 4, the three profiles and experimental results disagree. The *v2-f* model predicted a low intensity of turbulence that explains the slow velocity decay provided by this model. The two *k-ε* models agreed better with experimental results. The standard *k-ε* predicted the maximum turbulence intensity off-set and it presented lower values than the experimental data, whilst the realizable *k-ε* correctly predicted the position of maximum intensity.

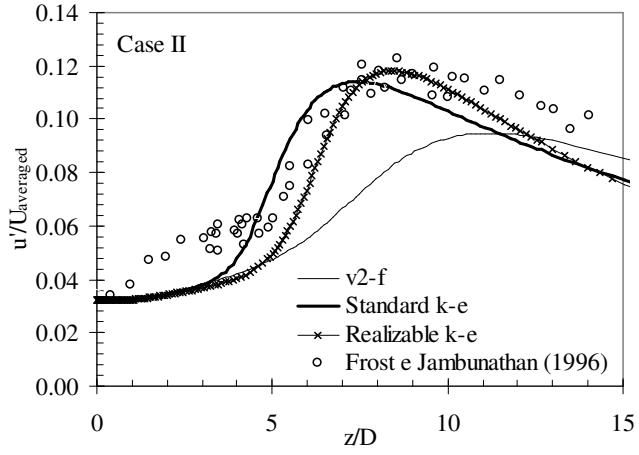

Figure 7. Case II – Intensity turbulence on symmetry axis vs. normalized distance from nozzle exit results of the three tested turbulence models.

Figure 8 shows turbulence intensity contour for the *v2-f* and the standard *k-ε* model. It can be verified that, in the jet border and close to symmetry axis, the turbulence intensity has almost the same values. However, in the region between border jet and symmetry axis there is a maximum value of turbulence intensity that is larger for the *k-ε* model than for the *v2-f* one. Based on these results, a preliminary analysis of an unknown problem can be performed where the

standard *k-ε* and the *v2-f* turbulence models can supply an insight about maximum and minimum turbulence intensity values.

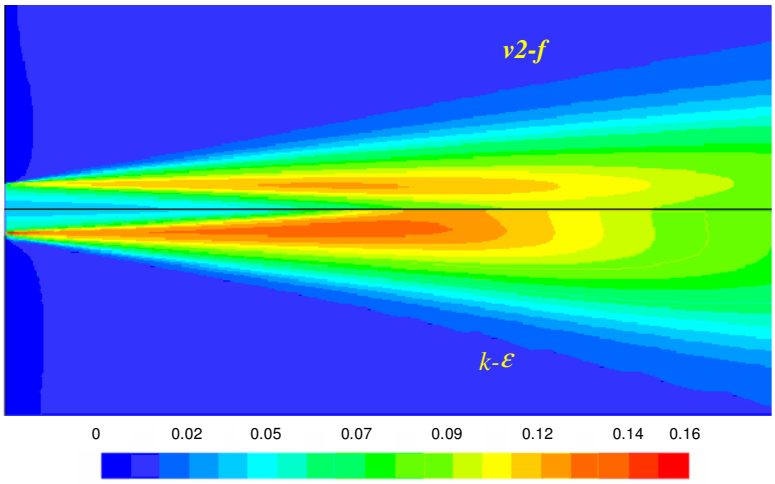

Figure 8. Case II - Predicted evolution of turbulent kinetic energy ($m^2\ s^{-2}$).

Summarizing, unlike the results of jet simulation with the 'top-hat' profile (Case I), both the realizable and the standard *k-ε* models didn't show good agreement with experimental data for the jet with the parabolic profile (Case II and III), which indicates that the models cannot properly account for the jet origin conditions. This feature, according to George and Davidson (2004) conclusions, shows that RANS models cannot correctly account for dependency on initial conditions, due to lack of required physics phenomena.

Many authors suggest the use of "problem function" or new values for the turbulence models constants, but this procedure unfortunately reduces even more the predictability of a turbulence model due to dependence on the problem. Some "problem functions" approaches for turbulent jets are given in Launder et al. (1972), McGuirk and Rodi (1977), and Morse (1977).

Figure 9 shows the numerical results obtained from the turbulence models with modified constants. In the standard *k-ε*, the constant $C_{\varepsilon 1} = 1.44$ was changed to 1.60, as suggested by Pope for round jets simulation. Calculations performed with this value of $C_{\varepsilon 1}$ provided a potential core length, which is in good agreement with experimental value (Senesh and Babu, 2005).

For the *v2-f* model, $C_{\varepsilon 1} = 1.3$ instead of $C_{\varepsilon 1} = 1.4$ was used as suggested by Durbin (1995) in the problem of plane mixing layers spreading rate. For the realizable *k-ε*, $C_{\varepsilon 2} = 1.8$ instead of $C_{\varepsilon 2} = 1.9$ was used.

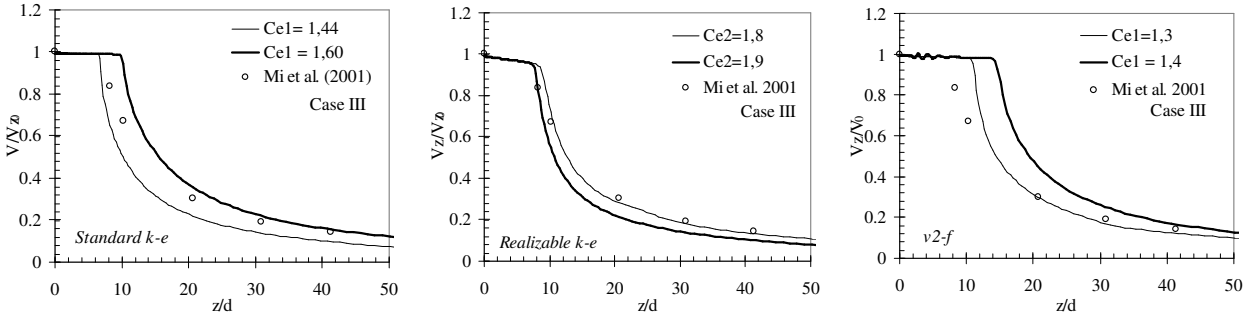

Figure 9. Case III - Normalized mean axial velocity on symmetry axis vs. normalized distance from nozzle exit results of the three tested turbulence models with modified and standard constants.

Figure 9 shows that the turbulence models constants can be 'calibrated' to improve the turbulence models agreement with results of previously known problems. However, these modified models become more and more constrained to predict a new problem behavior. For the standard *k- ε*, results suggest that the best value for $C_{\varepsilon 1}$ is between 1.44 and 1.60. Senesh and Babu (2005), using $C_{\varepsilon 1} = 1.56$ in the standard *k- ε*, obtained good results for subsonic free jet simulation (Mach = 0.6). The numerical data obtained from the modified realizable *k-ε* model gave the closest agreement to experimental data, whilst the modified *v2-f* model didn't agree with the data.

Results of this work provide additional evidence that the turbulence models coefficients are not absolute and that its constants are not universal. None coefficients set will provide the best estimation of all free jet regimes. As George (1989) argues, it is worse than simply needing different constants for axisymmetric and plane jets flows since each of these flows will require a multiplicity of constants to account for different starting conditions.

5. CONCLUSIONS

In the present study, the turbulent free jet problem with two different origin boundary conditions was numerically solved. Results obtained using the two tested k-ε turbulence models presented good agreement with experimental ones with "top-hat" jet origin boundary condition, while this behavior does not occur using the developed inlet profile. As mentioned in the literature, the model of constants adjustment improves results agreement for a specific problem. However, this procedure leads to a reduced predictive capability.

6. REFERENCES

Barth T. J. and Jespersen D., 1989, "The design and application of upwind schemes on unstructured meshes",Technical Report AIAA-89-0366, 27th Aerospace Sciences Meeting, Reno, Nevada.

Durbin, P. A., 1995, "Separated Flow Computations with the k-ε-v^2 Model", AIAA Journal, Vol.33, n.4, pp.659-664.

Frost, S. A., Jambunathan, K., 1996, Effect of nozzle geometry and semi-confinement on the potential core of a turbulent axisymmetric free jet, Int. Comm. Heat Mass Transfer, Vol. 23, n.2, p. 155-162.

George, W. K., 1989, "The Self-similarity of Turbulent Flows and its Relation to Initial Conditions and Coherent Structures", In Recent Advances in Turbulence (ed. R. E. A. Arndt & W. K. George), pp. 39-73.

George, W. K., 2004, Davidson L., 2004, "Role of Initial Conditions in Establishing Asymptotic Flow Behavior", AIAA Journal, Vol.47, pp. 438-446.

H. Schlichting, 1979, "Boundary Layer Theory", seventh ed., McGraw Hill, Nova York, pp. 700.

Launder, B. E., Spalding, D. B., 1972, "Lectures in Mathematical Models of Turbulence", Academic Press, London, England.

Mcguirk, J. J., Rodi, W., 1977, The Calculation of Three-Dimensional Free Jets, Symposium on Turbulent Shear Flows, Pennsylvania State University.

Mi J., Nobes D. S., Nathan G. J., 2001, "Influence of jet exit conditions on the passive scalar field of an axisymmetric free jet", J. Fluid Mech. 2001, Vol. 432, pp. 91-125.

Mi, J., Nathan, G.J., Nobes, D.S., 2001, "Mixing Characteristics of Axisymmetric Free Jets From a Contoured Nozzle, an Orifice Plate and a Pipe", Journal of Fluids Engineering, ASME Vol. 123, pp. 878-883.

Morse, A. P., 1977, Axisymmetric Turbulent Shear Flows with and without Swirl, Ph. D. Thesis, London University, England.

Pope, S. B., 1978, "An Explanation of the Round Jet/Plane Jet Anomaly", AIAA Journal, Vol. 3, pp. 279-281.

Pope, S. B., 2005, "Turbulent Flows" , Cambridge University Press, Cambridge, UK,771 p.

Schlichting H., Boundary – Layer Theory, seventh ed., McGraw – Hill, Nova York, 1979, pp 700.

Senesh, K., Babu, V., 2005, "Numerical simulation of subsonic and supersonic jets", American Institute of Aeronautics and Astronautics Paper AIAA-2005-3095, 11th AIAA/CEAS Aeroacoutics Conference.

Shih, T.-H., Liou, W. W., Shabbir, A., Yang, Z., and Zhu, J. A, 1995, "A new k- ε eddy-viscosity model for high Reynolds number turbulent – lows - Model Development and Validation", Computers Fluids, Vol.24, n.3, pp.227-238.

Vandoormaal J. P., and Raithby G., D., 1984, "Enhancements of the SIMPLE Method for Predicting Incompressible Fluid Flows", *Numer. Heat Transfer*, Vol.7, pp. 147-163.

White, F. M., 1991, "Viscous Fluid Flow". McGraw-Hill, New York.

Wilcox, d. C., 1994, "Turbulence Modeling for CFD", DCW Industries.

7. RESPONSIBILITY NOTICE

The authors are the only responsible for the printed material included in this paper.